Sensors & Transducers, Vol. 201, Issue 6, June 2016, pp. 17-26

Sensors & Transducers

http://www.sensorsportal.com

Feasibility of Commercial Resistive Flex Sensors for Hand Tracking Applications

Giovanni SAGGIO, Antonio PALLOTTI, Laura SBERNINI, Vito ERRICO, Franco DI PAOLO

Dept. of Electronic Engineering, University of Rome "Tor Vergata", 00133 Rome, Italy
Tel.: 0039 06 72597260, fax: 0039 06 23314067
E-mail: saggio@uniroma2.it

Received: 2 May 2016 /Accepted: 6 June 2016 /Published: 30 June 2016

Abstract: Human hand is a masterpiece of mechanical complexity, and the measure of its motion capabilities can be a challenging matter. Currently, these measures are generally performed by standard-gold techniques which mostly rely on video-based systems, advantageously effective, but disadvantageously expensive and time-consuming. To overcome such limitations, different researchers have been proposing different and new technologies aimed at tracking the posture and motions of the hand. Unfortunately, these technologies are, for the most part, not commercially available, being based on prototypes of sensors. In such a frame, however, commercial resistive flex sensors can be considered as an off-the-shelf valid technological solution for those who want to realize a cost-effective tracking system of both fingers and wrist. These sensors have been already used and investigated by researchers but, as far as we know, no comprehensive investigation about their mechanical-electrical transduction and feasibility capabilities are reported. This work intends to fill this lack. *Copyright © 2016 IFSA Publishing, S. L.*

Keywords: Resistive flex sensor, Bend sensor, Hand tracking, Finger's joints tracking.

1. Introduction

The hands can be considered as the universal human interface, as we heavily interact with the surroundings through them. The hands are a masterpiece of mechanical complexity, so that their precise tracking is not a trivial matter. However, many efforts have been made to measure and to monitor the motion of the fingers and wrist, for a variety of reasons and usefulness. We can refer to evaluations of: hand rehabilitation following a surgical operation [1], motor skill performance of the hand in diseases [2], intuitive remote control of a anthropomorphic hand [3-4] or drone, intuitive-way for a human-computer interaction [5-6], dexterity assessment for surgeons [7], and so on.

The system of measurements of the human hand is required to have particular characteristics, among which a certain sensitivity, repeatability, durability and cost-effectiveness.

In the panorama of human hand tracking, different technologies have been utilized, such as the ones based on cameras [8-9], on fiber optics [10], on led-photodiode couples [11], on inertial measurement units [12-13], on capacitance-based devices [14], on inductive-based devices [15], on Hall-effect-based devices [16], etc. However, those technologies are for the most part research products rather than off-the-shelf ones.

End users, who want to measure hand motions, actually utilize mainly camera-based commercial products which, in general, do not allow an optimal trade-off between accuracy of the measure and cost-effectiveness, since cost grows exponentially with accuracy. Systems such

as the Vicon (www.vicon.com), the BTS (www.btsbioengineering.com) and the Optitrack (www.optitrack.com), which are currently considered as gold-standards, assure high accuracy, but are costly and time-demanding for their set-up too. Differently, end users can utilize low-cost systems, such as the Kinect sensors-based, together with the related Handpose software (by Microsoft) which has, anyway, a too poor accuracy for too many applications.

In such a panorama, here we intend to investigate the feasibility of commercial resistive flex sensors (RFSs), in particular for hand tracking applications. These type of sensors have been already adopted by several authors, examples in [5, 17-19], each underlying different aspects and possible applications, but without reporting a comprehensive investigation, that we intend to realize here, as an extension of a previous work [20].

2. Materials and Methods

An RFS consists of a conductive layer engineered on-top of a plastic bendable substrate. The conductive layer is generally made of a carbon-based ink which presents some micro-cracks. When the sensor is flexed those micro-cracks move away so that the electrical resistance increases. When the sensor returns to its initial flat condition those micro-cracks return to their initial state of separation, and the electrical resistance returns to the nominal (initial) value, being the procedure reversible. Some RFSs can present an additional layer on-top of the conductive one, which acts as a protection against environmental contamination, and the RFS is said over-laminated (or coated).

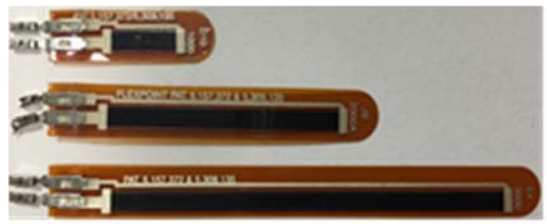

(a)

(b)

Fig. 1. (a) RFSs, by Flexpoint, with different length of 1", 2", 3" and (b) RFS, by SpectraSymbol, with additional metal squared pads visible on the top surface.

For this study, among different commercial RFSs, we selected the mostly adopted ones, which are furnished by Flexpoint (FP hereafter, www.flexpoint.com) and by SpectraSymbol (SS hereafter, www.spectrasymbol.com).

In particular, FP furnishes RFSs with different length and different over-laminations, so that we investigated sensors of 1, 2 and 3 inches in length (Fig. 1(a)) and with none-, polyamide-, polyester-overlamination (Table 1).

Differently, SS furnishes a unique type of RFS, having medal pads on-top of the conductive layer in order to reduce the nominal resistance. We adopted SS RFSs of 4.5 inches in length (Fig. 1(b), Table 1).

Table 1. Types of commercial RFSs we investigated, which are commercialized by Flexpoint and SpectraSymbol.

Flexpoint		
Code	***Overlamination***	***Length***
C5, H11, N7	none	1"
A15, B11, G6, H6, H15, I15, I17	none	2"
B10, D11, F16	none	3"
G5, G14, J4	polyester	2"
C1, C14	polyester	3"
A17, C15, I12	polyamide	2"
E3	polyamide	3"
SpectraSymbol		
S1, S2, S3	unknown	4.5"

These RFSs can be used for hand tracking applications, lying down them on each joint of each finger (Fig. 2), so to record electrical resistance variations in accordance of the flex-extension capabilities of the fingers.

Fig. 2. An RFS can measure the flexion/extension of the joint when lied down on-top of the joint itself. In this picture a FP RFS on-top of the proximal-interphalangeal joint of the index finger.

2.1. Set-up

In order to investigate the capabilities of the RFSs to convert mechanical bending variations into

electrical resistance variations, we designed and realized a specific set-up. In particular, each RFS, in turn, was lied down on an ad-hoc realized hinge made of two leafs, one fixed and the other rotating by means of a stepper motor (PD-109-57 by Trinamic, Hamburg, Germany) which moves the central pin linked to the rotating leaf (Fig. 3). The high precision (0.1 μm in tolerance) of the stepper motor assured that each imposed angle was correctly reached by the rotating leaf and, randomly, a visual inspection (within its limits), confirmed that the pre-imposed angle was reached, with respect to a reference goniometer.

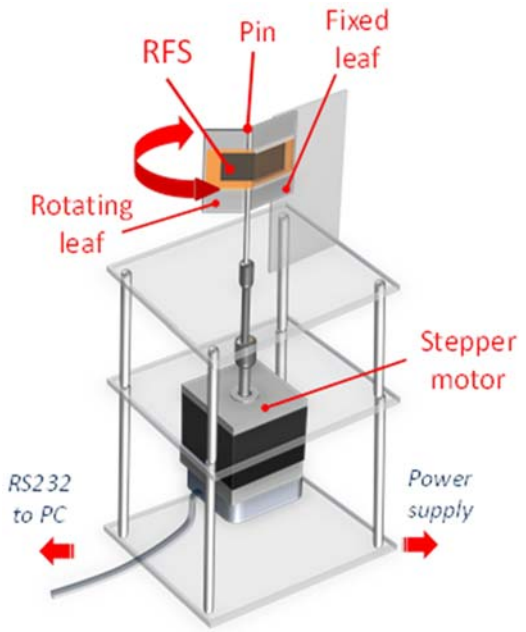

Fig. 3. The RFS lies on a hinge having one leaf rotated by means of a stepper motor.

2.2. Protocol

According to the literature, the maximum bending angle for a finger joint is less than 120° [21]. Therefore, neglecting hyperextension capabilities, we measured the electrical resistance R of each RFS versus the angle α of its bending, starting from an initial angle of 0° till a maximum angle of 120°.

Since the frequency motor capabilities of the hand is quite limited (fingers can open-close five times a second as maximum), we focused on a quasi-static characterization of each RFS. Accordingly, we stepped the 0°-120° range every 10°, with a resulting array of 13 angles α_i (i=0, 10, 20, …, 120), and at each 10° steps we assumed a 6s pause, so to collect and average 12 resistance values, measured with a millimeter (34405, by Agilent, Santa Clara, CA, USA). Consequently we had one resistance R_i (i=0, 10, 20, ... , 120) for each angle. The same procedure was repeated backwards, from 120° to 0°, and the 0°-120°-0° bending cycle was 10 times iterated for all sensors under test.

3. Results and Discussion

3.1. R vs. α

Fig. 4(a) shows points representing the couples R_i vs. α_i for the no-overlaminated (or uncoated) 2'' FP RFSs, and curves that interpolate those points. Differences among RFSs of the same type, which theoretically have to present equal responses, are conversely evident. This may suggest low repeatability in the process of manufacturing. The variation range of the resistance (ΔR), with bending angle within 0°-120°, is very different from ~145 kOhm of H6 sample (ΔR %≅2434 %), to ~446 kOhm of B11 sample (ΔR %≅4319 %). In spite of these differences, Fig. 4(b) shows that, if we normalize the resistance data to 0-1 range, the behavioral trend for all the sensors is practically the same.

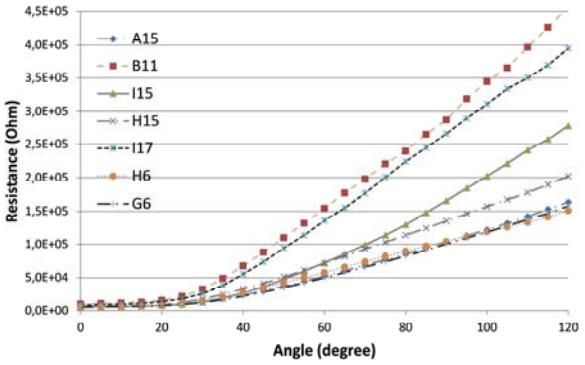

(a)

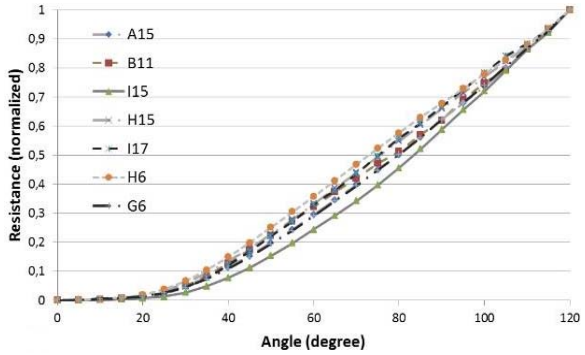

(b)

Fig. 4. R vs. α interpolated curves for each uncoated 2" FP RFS as (a) absolute and (b) normalized values.

This is also underlined in Fig. 5 reporting that, if we assume a unique normalized averaged curve for all the same type of samples, our error is practically null near 0° and 120°, with a maximum error value of ~13 % around 75°.

Measures showed that the same behavioral trend of the R vs. α curves, already seen for uncoated RFSs, is

also for polyamide-coated and polyester-coated FP samples (Fig. 6), which differ from variation range of the resistance (ΔR) anyway.

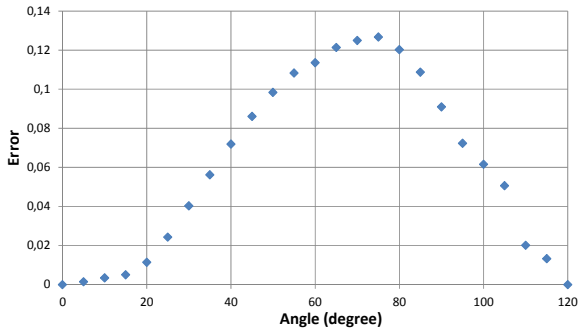

Fig. 5. The maximum differences in resistance between normalized curves at each angle of bending for the uncoated 2" FP RFSs.

In particular, for polyamide-coated samples, the resistance varies from ~51 kOhm of C15 sample (ΔR %≅401 %), to ~86 kOhm of A17 sample (ΔR %≅833 %). For polyester-coated samples, the resistance varies from ~95 kOhm of J4 sample (ΔR %≅1719 %), to ~111 kOhm of G5 sample (ΔR %≅1307 %).

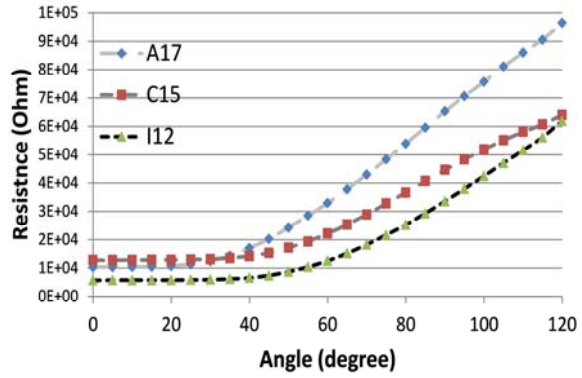

(a)

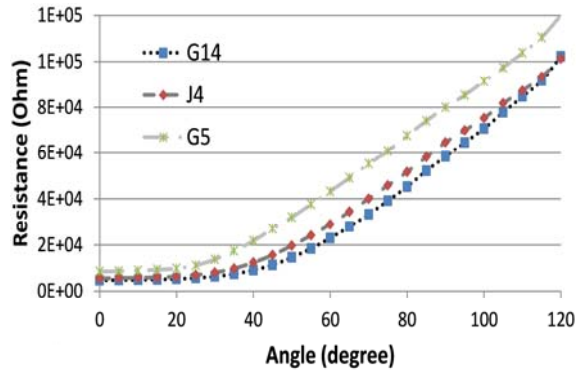

(b)

Fig. 6. R vs. α curves for FP (a) polyamide and (b) polyester samples.

Table 2 summarizes results obtained for the 2 inches FP samples. It is worth to note that the highest variation in resistance, with bending, belongs to the uncoated flex sensors with an average of 3538 % of increment when the sensors are 120° flexed with respect to the not-flexed (or flat) status. Differently, the polyester-coated and polyamide-coated versions demonstrate a lower average incremental variation of 1696 % and 740 %, respectively. This is due to the fact that the protective layer reduces the possibilities of the conductive layer to increment the micro-cracks distances with bending (the polyamide being more effective from this point of view). On the other hand, the polyester or the polyamide coatings offer a mechanical and environmental protection, which can be mandatory for some applications.

Table 2. Results obtained for 2" fp rfss: minimum and maximum values of resistance (rmin, rmax), variations of resistance in terms of absolute value, percentage value and averaged percentage value (Δ_{ABS}, $\Delta_{\%}$, $\Delta_{\%AVG}$).

Overl.	Code	Rmin [Ω]	Rmax [kΩ]	Δabs [kΩ]	Δ %	Δ% avg
None	H6	5952	150.8	144.9	2434	3538
	A15	5788	163.7	157.9	2728	
	G6	5522	158.0	152.5	2762	
	H15	6117	202.2	196.1	3205	
	B11	10333	456.6	446.3	4319	
	I17	8441	394.1	385.7	4569	
	I15	5734	278.1	272.3	4750	
Poly-amide	C15	12769	640.2	512.5	401	740
	A17	10333	964.0	860.7	833	
	I12	5713	619.5	562.4	984	
Poly-ester	G5	8532	120.1	111.5	1307	1696
	J4	5571	101.3	957.6	1719	
	G14	4736	102.3	975.7	2060	

As well as we already observed for uncoated samples, if we normalize the resistance data to 0-1 range, also the behavioral trends for the polyamide-coated and the polyester-coated sensors result similar (Fig. 7).

In order to find a useful and simple mathematical expression which could express the "R vs. α" curves, we tried mathematical interpolations by means of the *polyfit* function of Matlab (by MathWorks®, Inc.), that is a polynomial fitting. The related fit error was evaluated in terms of residuals, that is, differences between the response data and the fit to the response data. In Table 3, examples are reported for the cases of the A15 sample (no-overlaminated 2" FP), J4 sample (polyester-overlaminated 2" FP), and C15 sample (polyamide-overlaminated 2" FP). In particular, a 6th degree polynomial curve fitting has residuals as low as ~2.3 %, ~2.5 %, ~1.2 % for A15, J4, C15 samples, respectively, in comparison to a simpler linear approximation. A polynomial higher than 6th degree does not lower meaningfully those residuals. Anyway, the 6th degree polynomial claims the sensor to be subjected to a time-expensive calibration procedure before its usage, since it is necessary to bend it at six

different known angles and acquiring the relative resistance values to obtain the six coefficients of the equation.

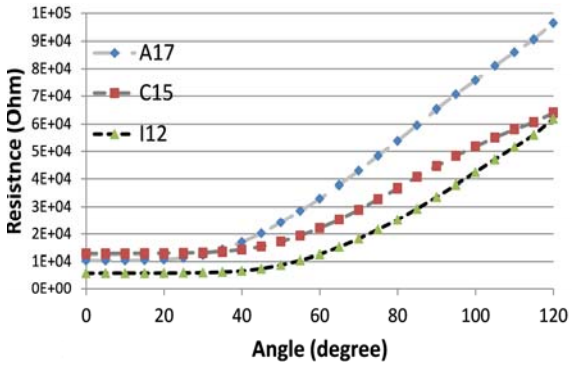

(a)

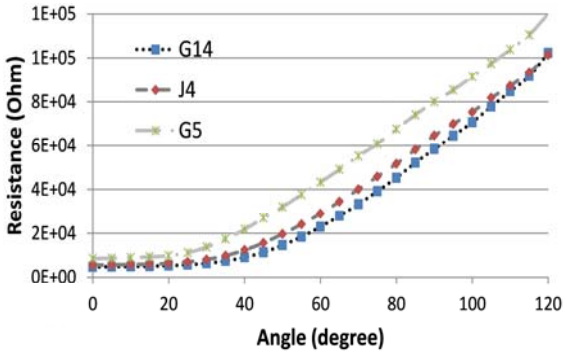

(b)

Fig. 7. R vs. α interpolated and normalized curves for each (a) polyamide-coated 2" FP RFS and (b) polyester-coated FP RFSs.

Table 3. Residuals with respect to the equation degree.

Equation degree	Residuals		
	A15	***J4***	***C15***
1st	54909	40757	28134
2nd	13240	10875	9129
3rd	4186	4367	5734
4th	3405	3863	2121
5th	2232	1220	1300
6th	1262	1014	345
7th	1127	983	310
8th	1115	882	275
9th	1012	871	176
10th	957	871	172

A convenient alternative way can result considering a step-wise linearization: a linear fitting within 0°-40° range and another linear fitting within 40°-120° range. In such a manner, the angle range versus R^2 couples "$\Delta\alpha$; R^2", being R^2 the coefficient of determination, results:

- sample A15: "0°-40°; 0.8275" and "40°-120°; 0.9962"
- sample J4: "0°-40°; 0.7878" and "40°-120°; 0.9963"
- sample C15: "0°-40°; 0.7977" and "40-120°; 0.9929"

Although these values are obtained for particular cases (i.e. for FP uncoated, polyester-coated and polyamide-coated 2" RFS samples), the same results can be usefully generalized for any FP RFSs, because of the possibility of normalization already mentioned.

When the non-linearity can be an issue, different authors propose different linearization procedures, such as the insertion of a standard fixed-value resistor in parallel to the RFS under test [22], or the cutting of the RFS in a shape different from the standard rectangular one [23] or, finally, the addition of a coating layer [22], but waiving to the advantage of the greater sensitivity and, de facto, tuning to the coated case.

Differently from the FP RFSs, the SS ones demonstrate an inner high degree of linearity (R^2=0.997), as showed in Fig. 8, where it is reported an average of the three samples (S1, S2, S3) under measure. It can be evidenced also a low standard deviation (SD), that implies a high degree of repeatability of the measure.

For the average of the three SS RFSs under examination, the resistance varies from ~11.6 kOhm to ~21.2 kOhm, with a variation of ~9.7 kOhm (ΔR %≅84 %), which is one and two order of magnitude lower than the polyamide-laminated FP and the polyester- and none-laminated FP, respectively.

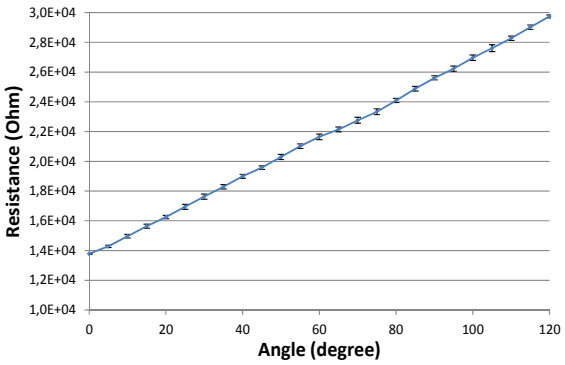

Fig. 8. The SpecrtaSymbol RFSs demonstrate an inner high degree of linearity of the "R vs. α" curve, and a low SD.

Accordingly to a previous work, the linear "*R* vs. α" trend of an RFS is due to isotropy of both the supporting layer and the on-top engineered sensible material [24]. This aspect suggests that FP RFSs have (at least partially) anisotropic material (Fig. 9), while SS RFSs have high isotropy of the layers.

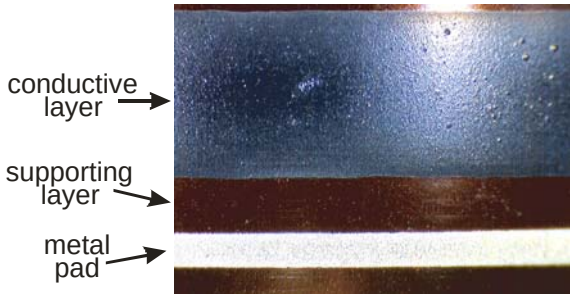

Fig. 9. A 20× optical image of the A15 sample, that is 2" no-overlaminated FP RFS.

3.2. Sensitivity

The polyamide-laminated, polyester-laminated and no-overlaminated FP RFSs gain higher sensitivity, $S=\Delta R/\Delta\alpha$, for angles >40°, >25° and >18° respectively, as reported in Fig. 10.

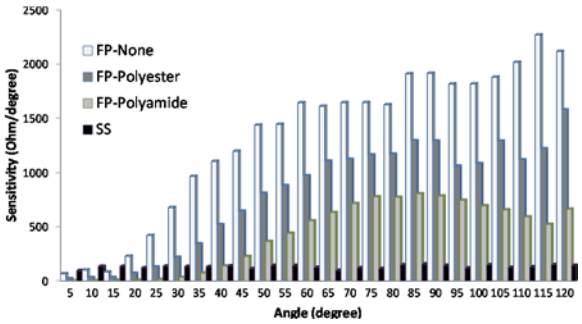

Fig. 10. Sensitivity versus bending angle for all types of RFSs.

For lower angles the FP RFSs sensitivity is reduced and comparable to the one of the SS RFSs.

3.3. Repeatability and Hysteresis

Among the specific features of an RFS, it is important that such a sensor can perform without any meaningful variation in response when subjected to the same testing conditions, i.e., offer repeatability. In addition, it is relevant to observe if the resistance value acquired at the same angle is maintained without meaningful hysteresis, that is, when tests are performed when the stepper motor both increases or lowers the angle values.

All our tests were ten times iterated, and we evaluated the repeatability of the measures in terms of the standard deviation (SD) expressed in percentage. Fig. 11 summarizes the obtained results.

It can be evidenced that a lower, and practically constant SD(%) results for the SS RFSs at all the tested angles. The FP RFSs perform with higher SD(%) in particular for middle angles, and the coated versions perform with higher SD(%), therefore a lower repeatability.

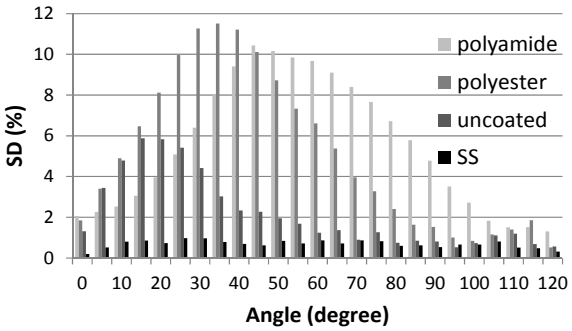

Fig. 11. SD(%) versus bending angle for all types of RFSs.

Regarding the hysteresis, all RFSs performed with values lower than the respective SD, so that we can affirm that it is practically irrelevant.

3.4. R vs. Pin Radius

The resistance variation in bending an RFS is necessarily proportional to the portion of its length effectively flexed. Therefore, it is reasonable to experience higher resistance variation for lower value in diameter of the pin of the hinge in our measurement set-up (by extrapolating we can say that an infinite diameter pin corresponds to a not-flexed sensor, so no-variation of its resistance). Fig. 12 reports the resistance trend for the special case of the FP RFS B11 sample measured on-top of four different pins of 0.6 cm, 0.8 cm, 1.0 cm and 1.2 cm in diameter, respectively. Although this is just an example, we experienced the same trend for all our FP RFSs samples.

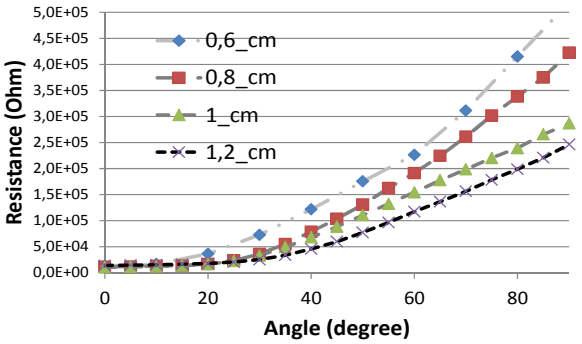

Fig. 12. Comparison of resistance variation trends of the FP B11 sample when flexed around pins with different diameter.

We wat to point out that our interest was focused on RFSs application in tracking of movements of the fingers, so that those diameters of the pins should represent the average diameters of the joints of the human fingers, but they don't actually. We made a hard work to find a research work reporting averages of the anthropomorphic measures of the human fingers' joints, but we did not find any satisfactory results. Therefore, we considered that the diameters of

the joints are roughly similar to that of the fingers (with the exception of metacarpo-phalangeal joint which is slightly larger), and those diameters can be obtained by the finger-size system used for selling wedding rings. As averages, the diameter for the ring finger is about 1.63 cm for woman and 1.96 cm for man. These measures can be an indication for the other fingers too but, anyway, are larger with respect to the diameters of the pins that we have. Nevertheless, the results we obtained are meaningful, demonstrating a clear tendency.

3.5. Different Coatings

An additional layer, on-top of the conductive one, can help in mechanical protection and increase the possible cycle of bending mechanical stress before failure of the sensor. This is why some types of RFSs come with coatings, in particular made of polyester or polyamide. Anyway, the advantages resulted from a mechanical point of view affect the sensors electrical performances. In particular, our tests evidenced a reduction in the range (max-min) of resistance variation, more evident with the polyamide coating with respect the polyester one (see Table 4).

Regarding the SS RFSs, those sensors resulted with the lower range, possibly due to the metallic pads, since there is no evidence of a coating (no mentioned on the datasheets).

Again, in spite of the coating layer, the FP RFSs result with the same trend in "R vs. α" curves, as evidenced in Fig. 13 which reports the normalizing resistance data to 0-1 range.

Table 4. Comparison of min, max and range of average resistance values of different RFSs.

RFS type	Resistance [Ohm]		
	min	***max***	***range***
Uncoated FP	6839	257756	250917
Polyester-coated FP	6279	107904	101625
Polyamide-coated FP	9605	74124	64519
SpectraSymbol	13783	29750	15967

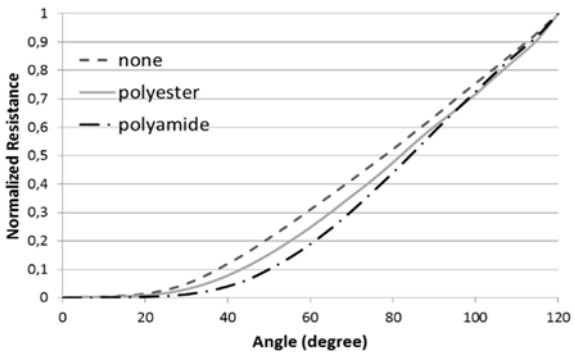

Fig. 13. Normalized resistance versus bending angle for FP RFSs differently over-laminated.

3.6. Outward Bending

For completeness, in addition to the outward bending (that is, the bending which "elongates" the sensible conductive layer), we performed the inward bending (that is, the conductive layer is shortened), in particular from 0° to -90°, 5° stepped, averaging data of ten iterations. As it can be expected, results demonstrated the uselessness of RFSs in inward flexion.

As an example, Fig. 14 reports the behavior of the C1 (polyester-coated 3" in length) FP RFS sample.

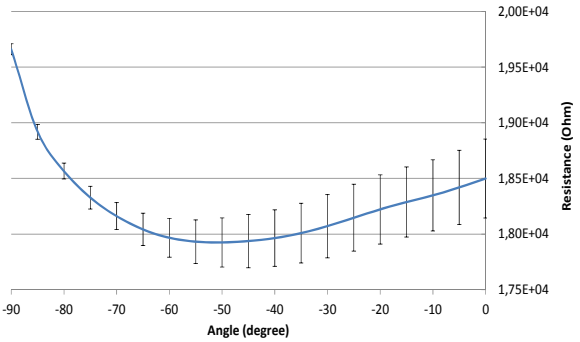

Fig. 14. How FP C1 sample behaves in inward bending. High vertical lines evidence high value of SD.

This figure shows a non-monotonic function, which leads to the impossibility to determine unequivocally a bending angle from the reading of the resistance of the sensor. In addition, it can be evidenced an inconsistent repeatability of the measure, since too high standard deviation values, in particular for angle of bending within the -70° and 0° interval.

3.7. Step Response Decay & Time Decay

A common requirement for any sensor is that its response has to be always the same with unchanging boundary conditions, i.e. it has to be "stable vs. boundary". In addition, a time-independent sensor has to maintain its response unchanged with time, i.e. it has to be "stable vs. time". In order to evaluate this characteristic regarding our RFSs, we tested their step response decay (a variation in resistance over time after a step transition to a different bending angle).

Fig. 15 reports the obtained results. In particular, approximately 15 mins are necessary for the FP polyamide-coated, for the FP polyester-coated and for the SS RFSs to gain a roughly stable value of resistance, respectively equal to the 93 %, 90 % and 90 % of their initial value; three times that time (45 mins) occurs for the FP uncoated RFS to reach some stability in resistance equal to the 82 % of the initial value. These results are comparable to the ones obtained in [26], and suggest that it is fundamental to

establish always the same acquisition time after each bending of the sensors.

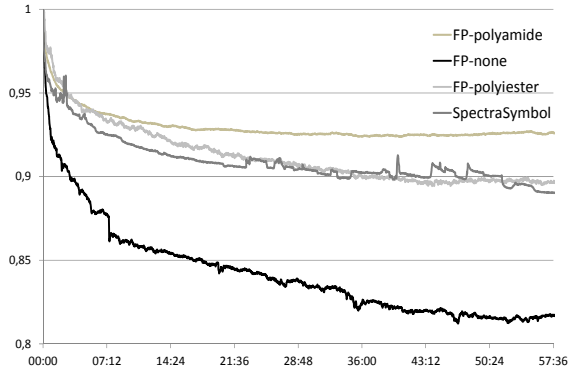

Fig. 15. Step response decay, during 60min, for all RFSs under test.

In order to consider differences in performances vs. time, we performed the same protocol of measurement four times within six weeks, that is, one every 14 days. Results are reported in Fig. 16, which evidences decays in performance, since ΔR values lower over time. This means that it is necessary to re-test the RFSs periodically.

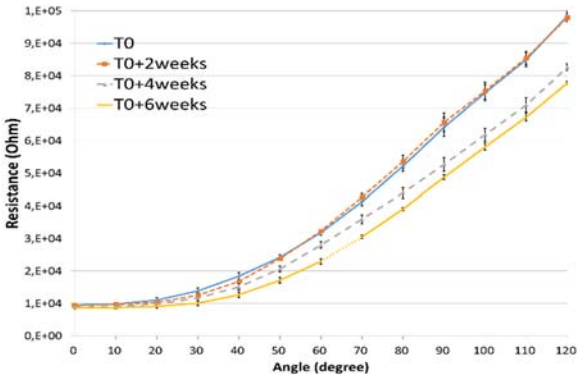

Fig. 16. One FP RFS characterized over a period of six weeks. The responses are different and show a decay.

4. Application to the Sensory Glove

Because of the dimensions of the RFSs, one of the most convenient ways to adopt them is on-top of the joints of the fingers, so to measure the hand's motor capabilities. This is one of the potential applications of the RFSs, for a complete survey of the other applications the interested reader can refer to [26].

We housed 14 sensors into sleeves sewn on the dorsal aspect of a Lycra® glove, in the correspondence of the distal-interphalangeal (DIP), proximal-interphalangeal (PIP), metacarpo-phalangeal (MCP) joints of the index, middle, ring, pinky fingers and the inter-phalangeal (IP) and metacarpo-phalangeal (MCP) joints of the thumb. As an example, here we report the case of a unique RFS placed in correspondence of the PIP of the index finger (Fig. 17), and its resistance outputs (Fig. 18).

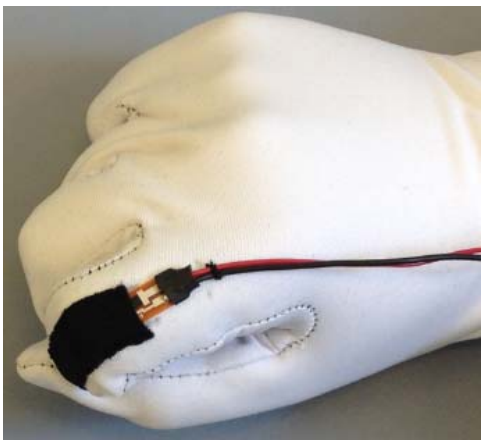

Fig. 17. The A17 sensor, which is a 2" polyamide-laminated FP RFS, placed in correspondence of the PIP joint of the index finger, being housed into a sleeve sewn onto a supporting glove.

Fig. 18 refers to the output of the sensor when the hand performs the opening/closing procedure without pausing. Despite the absence of pauses, the figure shows a sort of "plateau" near the x-axis. This evidences the non-linear behavior of the sensors that offers lower resistance variations for bending angles within the 0°-40° range.

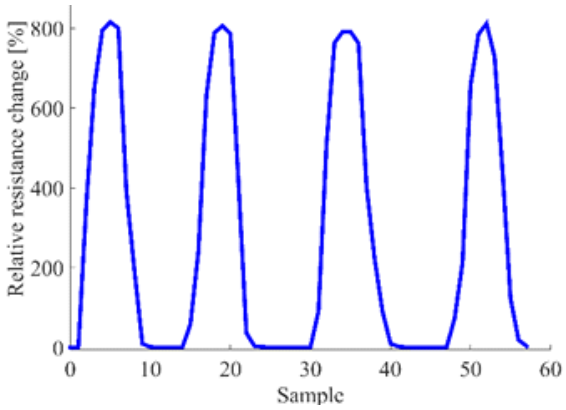

Fig. 18. Output of the A17 Flexpoint sensor with opening/closing circles of the hand. The sensor experiences about a 0°-120°-0° bending.

5. Conclusions

The different FP RFSs showed different "R vs. α" curves, but all of them with a common trend mathematically evidenced by a unique polynomial function. In particular, their resistance variation is lower for lower bending angle (< 40°) and increases, almost linearly, at higher angle (< 120°, > 40°).

This non-linear behavior can be considered as a disadvantage for some applications, but can be ineffective, or even profitable, for others. As an example, we can adopt FP RFSs in a sensory glove to convert angular displacement of the fingers into electrical signals. In such a case, when the glove is used to remotely control a prosthetic hand (mapping one-to-one the human movements with the electro-mechanical hand), the linearity of the sensor can be mandatory for high precision interventions. Differently, when the sensory glove is used for human-computer interactions (for instance to virtually grab objects on a video), the lower response of the FP RFSs at lower bending angle does not represent a relevant problem.

FP RFSs show a non-linear sensitivity too, which increases with angle of bending, and offer good repeatability without meaningful hysteresis value.

There are significant differences among RFSs with respect to their over-laminations. In particular, our experiments evidenced that uncoated RFSs present the greatest variations in resistance when flexed, the highest sensitivity and the lowest standard deviation. On the other hand, the absence of a protective layer reduces their mechanical stability.

Finally, FP RFSs show decays in performances over time.

Differently, SS RFSs demonstrated linearity, but a meaningful lower resistance variation with bending.

None of the sensors offer a useful response in inward bending (i.e. when the sensible layer is shortened), and all sensors suffer from a step response decay.

As a conclusion, we can affirm that all RFSs we investigated can be usefully used to measure finger's flexion/extension, but the type of the sensor to be selected depends on the particular application.

Acknowledgment

This paper was partially based on a work supported by the Italian Space Agency (ASI), contract #2013-081-R0, for which we would like to thank Prof. Mariano Bizzarri, Dr. Simona Zoffoli and Dr. Francesca Ferranti.

References

[1]. G. Saggio, M. De Sanctis, *et al.*, Long Term Measurement of Human Joint Movements for Health Care and Rehabilitation Purposes, in *Proceedings of the 1th International Conference on Wireless Communications, Vehicular Technology, Information Theory and Aerospace & Electronic Systems Technology (VITAE'09)*, Aalborg, Denmark, 2009, pp. 674-678.

[2]. F. Cavallo, D. Esposito, *et al.*, Preliminary evaluation of SensHand V1 in assessing motor skills performance in Parkinson Disease, in *Proceedings of the IEEE International Conference on Rehabilitation Robotics (ICORR)*, 2013, pp. 1-6.

[3]. G. Saggio, M. Bizzarri, Feasibility of Teleoperations with Multi-Fingered Robotic Hand for Safe Extravehicular Manipulations, *Aerospace Science and Technology*, Vol. 39, 2014, pp. 666-674.

[4]. A. M. Zaid, M. A. Yaqub, UTHM HAND: performance of complete system of dexterous anthropomorphic robotic hand, *Procedia Engineering*, Vol. 41, 2012, pp. 777-783.

[5]. R. Berlia, P. Santosh, Mouse Brace: A convenient computer mouse using accelerometer, flex sensors and microcontroller, in *Proceedings of the Conference on Contemporary Computing and Informatics*, 2014, pp. 558-561.

[6]. T. Mohammad, H. Seifi, J. Shi, Design of gesture based input devices for controlling presentation, PhD Thesis, *The British Columbia University*, 2010.

[7]. G. Saggio, A. Lazzaro, *et al.*, Objective Surgical Skill Assessment: An Initial Experience by Means of a Sensory Glove Paving the Way to Open Surgery Simulation?, *Journal of Surgical Education*, Vol. 72, Issue 5, 2015, pp. 910-917.

[8]. V. F. Pamplona, L. A. Fernandes, J. Prauchner, L. P. Nedel, M. M. Oliveira, The image-based data glove, in *Proceedings of the 10th Symposium on Virtual and Augmented Reality*, 2008.

[9]. J. Choi, J. I. Park, H. Park, Twenty-one degrees of freedom model based hand pose tracking using a monocular RGB camera, *Optical Engineering*, Vol. 55, Issue 1, 2016, pp. 013101.

[10]. E. Fujiwara, C. Y. Onaga, M. F. Santos, E. A. Schenkel, C. K. Suzuki, Design of a glove-based optical fiber sensor for applications in biomechatronics, in *Proceedings of the 5th IEEE RAS & EMBS International Conference on Biomedical Robotics and Biomechatronics*, 2014, pp. 786-790.

[11]. L. Wang, T. Meydan, P. Williams, K. T. Wolfson, A proposed optical-based sensor for assessment of hand movement, *IEEE Sensors*, 2015, pp. 1-4.

[12]. P. C. Hsiao, S. Y. Yang, B. S. Lin, I. J. Lee, W. Chou, Data glove embedded with 9-axis IMU and force sensing sensors for evaluation of hand function, in *Proceedings of the IEEE 37th Annual International Conference on Engineering in Medicine and Biology Society*, 2015, pp. 4631-4634.

[13]. B. Fang, D. Guo, F. Sun, H. Liu, Y. Wu, A robotic hand-arm teleoperation system using human arm/hand with a novel data glove, in *Proceedings of the IEEE International Conference on Robotics and Biomimetics*, 2015, pp. 2483-2488.

[14]. N. Karlsson, B. Karlsson, P. Wide, A glove equipped with finger flexion sensors as a command generator used in a fuzzy control system, in *Proceedings of the IEEE Instrumentation and Measurement Technology Conference*, Vol. 1, 1998, pp. 441-445.

[15]. T. Kuroda, Y. Tabata, A. Goto, H. Ikuta, M. Murakami, Consumer price data-glove for sign language recognition, in *Proceedings of the 5th Int. Conference Disability, Virtual Reality Assoc. Tech.*, Oxford, UK, 2004, pp. 253-258.

[16]. O. Portillo-Rodríguez, C. A. Avizzano, E. Sotgiu, S. Pabon, A. Frisoli, J. Ortiz, M. Bergamasco, A wireless bluetooth dataglove based on a novel goniometric sensors, in *Proceedings of the 16th IEEE International Symposium on Robot and Human Interactive Communication*, 2007, pp. 1185-1190.

[17]. B. Debs, E. Mousallem, A. Hage-Diab, M. Hajj-Hassan, *et al.*, A Finger Movement Evaluation Device to Monitor the Use of Paretic Hand During Daily Life Activities, in *Proceedings of the 4th International*

Conference on Global Health Challenges, France, 2015, pp. 45-49.
[18]. D. Dutta, B. Champaty, K. Pal, I. Banerjee, Finger movement based attender calling system for ICU patient management and rehabilitation, in *Proceedings of the IEEE International Conference on Circuit, Power and Computing Technologies*, 2014, pp. 394-397.
[19]. A. Jacob, W. N. W. Zakaria, M. R. B. M. Tomari, Quantitative Analysis of Hand Movement in Badminton, in Advanced Computer and Communication Engineering Technology, *Lecture Notes in Electrical Engineering*, Vol. 362, 2016, pp. 439-448.
[20]. G. Saggio, A Comprehensive Investigation of the Electrical Features of Commercial Resistive Flex Sensors, in *Proceedings of the The 1st International Conference on Advances in Sensors, Actuators, Metering and Sensing (ALLSENSORS'16)*, 2016, pp. 40-45.
[21]. J. D. Arbuckle, D. A. McGrouther, Measurement of the arc of digital flexion and joint movement ranges, *The Journal of Hand Surgery: British & European Volume*, Vol. 20, Issue 6, 1995, pp. 836-840.
[22]. R. Gentner, J. Classen, Development and evaluation of a low-cost sensor glove for assessment of human finger movements, *J. Neurosci. Methods*, Vol. 178, Issue 1, 2009, pp. 138-147.
[23]. G. Saggio, Electrical resistance profiling of bend sensors adopted to measure spatial arrangement of the human body, in *Proceedings of the 4th Int. Symp. on Applied Sciences in Biomedical and Communication Technologies (ISABEL'11)*, 2011.
[24]. G. Saggio, Mechanical model of flex sensors used to sense finger movements, *Sensors and Actuators A*, Vol. 185, 2012, pp. 53-58.
[25]. N. P. Oess, J. Wanek, A. Curt, Design and evaluation of a lowcost instrumented glove for hand function assessment, *Journal of Neuroengineering and Rehabilitation*, 2012.
[26]. G. Saggio, F. Riillo, L. Sbernini, L. R. Quitadamo, Resistive flex sensors: a survey, *Smart Materials and Structures*, Vol. 25, Issue 1, 2016, pp. 1-30.